

Simulation and Fabrication of Soft Robots with Embedded Skeletons

James M. Bern¹, Fatemeh Zargarbashi², Annan Zhang¹, Josie Hughes² and Daniela Rus¹

Abstract—Soft robots can be incredibly robust and safe, but typically fail to match the strength and precision of rigid robots. However, this dichotomy between soft and rigid is starting to break down, with emerging research interest in hybrid soft-rigid robots. In this work we draw inspiration from nature, which achieves the best of both worlds by coupling soft and rigid tissues—like muscle and bone—to produce biological systems capable of both robustness and strength. We present foundational, general-purpose pipelines to simulate and fabricate cable-driven hybrid soft-rigid robots with embedded skeletons, and show that robots built using these methods can fluidly mimic biological systems, while also achieving greater force output and external load resistance than purely soft robots. Finally we show how our simulation and fabrication pipelines can be leveraged to create more complex hybrid robots, and do model-based control.

I. INTRODUCTION

Robots built from soft materials promise to be exceptionally robust [1] and safe [2]. Unfortunately, these benefits come at the cost of strength and precision, which is why robots that must carry large payloads [3], or operate with great precision [4], are typically traditional rigid designs. However, perhaps the future of high-performance robots does not be so black and white, soft versus rigid. Nature has found ways to exquisitely marry soft and rigid tissues, creating biological systems that are simultaneously robust, safe, strong, and precise [5].

Recently, robotics researchers have also demonstrated very promising results by combining soft and rigid elements. Iconic examples include a rigid robot arm outfitted with jamming gripper capable of picking up an enormous variety of objects [6], and a rigid-bodied robot with soft undulating cuttlefish-like fins that can traverse ground, water, and ice [7]. This space of hybrid soft-rigid robots is still in its early days of exploration, and promises to be incredibly rich. It includes soft-bodied robots that employ a more typically “rigid” actuation strategy—like the soft quadruped with rigid rotational joints in [8]—and rigid-bodied robots that employ a soft actuation strategy—like the tube-footed robots in [9]—as well as robots that are harder to classify—like the soft cheetah in [10], which features a rigid and soft body, with a rigid articulated spine, a spring, and pneumatic actuation.

In this work we aim to augment the robustness of a soft-bodied robot with the strength of a skeleton, and achieve

delicacy of control via multiple independently-actuated cables. Alternative approaches would be achieving strength through cables alone [11], or control via multiple pneumatic chambers [12]. However these approaches are limited respectively by the softness of the material, and the bulk of pneumatic actuation—where the chamber must serve as both actuator and body [13]. We follow in the footsteps of an array of robotics researchers who have drawn inspiration from animal and human skeletons [14]. This includes work on rigid human skeletons instrumented with soft actuators [15], [16], cable-driven skeletons with separately 3D printed soft body segments [17], pneumatically actuated soft fingers containing bones [18], a manipulator with a compliant spine [19], passive hands utilizing anthropomorphic bone structures [20], [21], and jamming joints [22].

Embedded skeletons bring the benefits of strength [23], [24] and precision, but they also add additional complexity. If we are to fully understand and harness the capabilities of soft robot skeletons, we need general purpose pipelines to simulate and fabricate them. Approaches to simulating hybrid robots include considering the robot as a series of rigid links [18], as well as employing an empirical anatomical model of tendon-driven finger motion [17]. To capture a wider array of hybrid soft-rigid robots, we employ a differentiable simulator based on the finite element method (FEM) [25]. FEM-based simulators have shown great promise for modeling and controlling more complex soft robots [19], [26]. This fact that our particular simulator is differentiable enables its use in model-based control methods like soft robot inverse kinematics (Soft IK) [27] and trajectory optimization [25].

Taken together, our pipelines for simulation and fabrication form a first comprehensive solution to design, fabricate, and model soft robots with internal skeletal system. This new breed of hybrid soft-rigid robots promises to be capable of mimicking biological systems—like the human body—with higher fidelity, while also 1) resisting larger external loads, and 2) performing tasks requiring greater strength. We contribute:

- A pipeline for simulating soft robots with skeletons, based on the finite element method.
- A pipeline for fabricating soft robots with skeletons, based on silicone casting.
- Real-world and simulated experiments to characterize the impact of skeletons on soft robot deformation behavior.
- Example applications including multi-finger grasping and single-finger trajectory optimization.

II. SIMULATION PIPELINE

Our simulation pipeline takes a design for a hybrid soft-rigid robot and generates a corresponding physically-based simulation from which we can predict the robot’s deformation

¹James M. Bern, Annan Zhang, and Daniela Rus are with the Computer Science and Artificial Intelligence Laboratory, MIT. jamesmbern@gmail.com, zhang@csail.mit.edu, rus@csail.mit.edu

²Fatemeh Zargarbashi and Josie Hughes are with the Computational Robot Design & Fabrication Lab, EPFL. fatemeh.zargarbashi@epfl.ch, josie.hughes@epfl.ch

© 2022 IEEE. Personal use of this material is permitted. Permission from IEEE must be obtained for all other uses, in any current or future media, including reprinting/republishing this material for advertising or promotional purposes, creating new collective works, for resale or redistribution to servers or lists, or reuse of any copyrighted component of this work in other works.

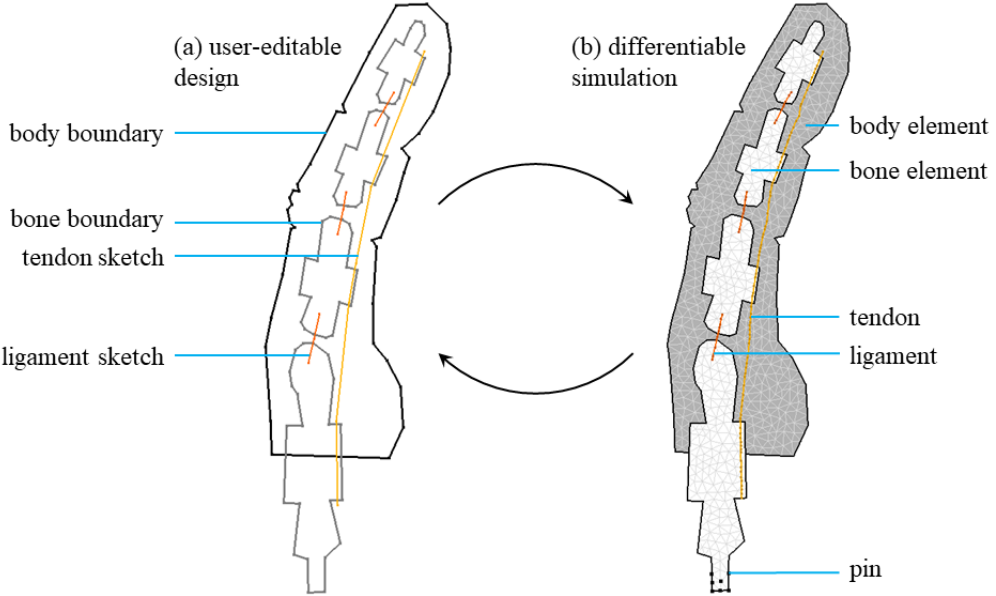


Fig. 1. We employ an iterative design and simulation pipeline. A user designs a robot by dragging around points defining the boundaries of body and bones, as well as the layout of the tendons and ligaments. Our system automatically generates a differentiable, FEM-based simulation from this design. This simulation can be employed as an exploratory tool to inform further design edits.

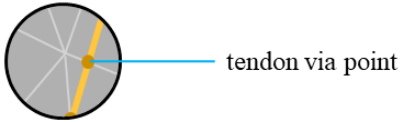


Fig. 2. Detail of the simulation in Figure 1. Via points (dark yellow dots) are automatically inserted where cable sketches cross finite element boundaries (light gray line segments). These via points help model a cable running through the silicone body of the robot.

and do model-based control. Our automated pipeline enables a user to toggle back and forth between design and simulation on the fly while making edits. Our differentiable simulator is based on the finite element method, and follows the same approach as [11], [25], [27]. Figure 1 has an example of a soft robot design and its corresponding simulation.

A. Design

A robot design consists of the boundary of the robot's soft body, the boundaries of the robot's bones, and the layout of the robot's cables (tendons and ligaments). For 2D simulations we define boundaries using a polygonal line loops, and for 3D simulations we use the faces of bounding volumes. In both 2D and 3D the tendon and ligament layouts are defined using a set of polylines we call *sketches*. In 2D we give the user the ability to quickly and intuitively make edits, by dragging around the boundaries and cable layout with the mouse. To convert the design into a simulation, we first discretize the body and bone boundaries into a finite elements mesh. We use Triangle [28] to triangulate 2D simulations, and TetGen [29] to tetrahedralize 3D simulations. We can automatically identify via points (see Figure 2) where the cable polylines cross the boundaries of finite elements using a small custom routine.

With the finite elements and cables thus defined, we do some final post-processing. We automatically assign Young's moduli to the finite elements—based on whether they are part of the body or the bones—and similarly assign spring constants to the cables and ligaments. Finally we add zero length spring pins to model boundary conditions, e.g. pinning the bottom nodes of the simulation in place to model a real-world robot being secured to the ground.

B. Simulation

We solve physics by using Newton's method to minimizing the total energy of the system U with respect to the positions of all nodes in the finite element mesh \mathbf{x} . This is the approach taken in [25], and can be used to simulate either statics or dynamics. Here we summarize the approach for statics. Formally, if we call the vector of control inputs \mathbf{u} , then the resulting statically stable shape of the robot is

$$\mathbf{x}^*(\mathbf{u}) = \arg \min_{\mathbf{x}} U(\mathbf{u}, \mathbf{x}). \quad (1)$$

The work energy principle has the expression for the nodal forces $\mathbf{F} = -\frac{\partial E}{\partial \mathbf{x}}$, which means $\mathbf{x}^*(\mathbf{u})$ solves $\mathbf{F}(\mathbf{u}, \mathbf{x}) = 0$.

We employ a Neo-Hookean material model, with per element energy density

$$\Psi(\mathbf{x}, \mathbf{X}) = \frac{\mu}{2} \text{tr}(\mathcal{F}^T \mathcal{F} - \mathbf{I}) - \mu \ln J + \frac{\lambda}{2} (\ln J)^2, \quad (2)$$

where \mathbf{X} is the rest shape, \mathcal{F} is the deformation gradient, $J = \det \mathcal{F}$, and λ and μ are material parameters. The material parameters can be expressed in terms of Young's modulus E and Poisson's ratio ν . To model a robot made by casting rigid bones inside of a soft silicone body, we assign Young's modulus E_{rigid} to elements making up the bones, and a softer Young's modulus E_{soft} to elements making up the robot's soft

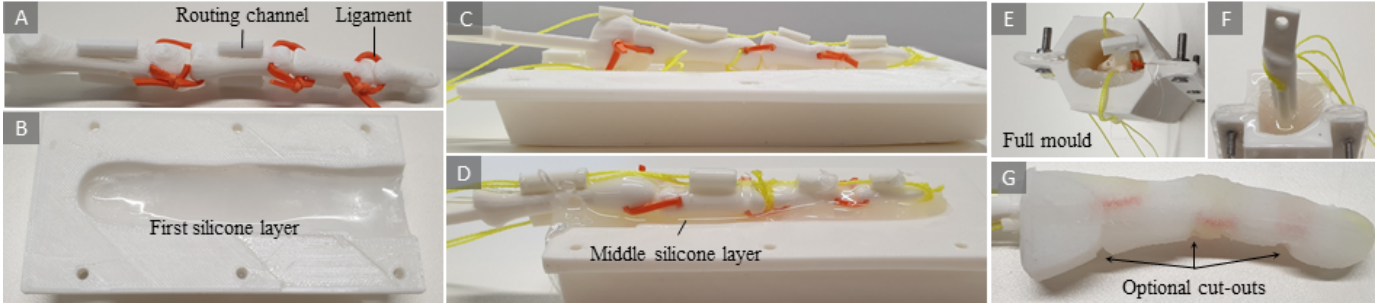


Fig. 3. We employ a multi-step casting process. We first (a) assemble the bones and ligaments, routing cables through the printed channels, then we (b) cast a first layer of silicone, (c) affix the skeleton assembly to the cured silicone layer, (d) apply an additional layer of silicone to keep the skeleton in place, (e) assemble the entire mould, and (f) pour the last layer of silicone. For our Dragon Skin examples we can (g) add cuts after demoulding to reduce stiffness.

body. To model self-collision events—like those taking place on the surface of knuckle cut-outs in Figure 4—we employ a 2D version of Li et al.’s IPC [30].

We consider cables and ligaments as polylines running through frictionless via points in the mesh. We model the energy stored in a tendon or ligament as a unilateral spring

$$U_{\text{cable}}(\mathbf{x}) = kQ(\ell(\mathbf{x}) - L), \quad (3)$$

where k is the spring constant, $\ell(\mathbf{x})$ is cable the length when the mesh has shape \mathbf{x} , and L is the rest length. The function Q is a one-sided quadratic defined such that the cable is slack under compression and follows Hooke’s law under tension [27]. Cables are given stiffer spring constant k_{cable} , and ligaments softer spring constant k_{ligament} . To model the action of a motor pulling some length of cable u onto a spool, we add $-u$ to the simulated cable’s rest length. We call u the cable’s *contracted length*. Ligaments cannot be actuated, and so we leave their rest length constant. We can slightly pretension this rest length to help model how ligaments hold bones more closely together during fabrication.

III. FABRICATION PIPELINE

We fabricate hybrid soft-rigid robots with skeletons like the finger in Figure 4 using the multi-step casting process outlined in Figure 3. Bones are printed out of PLA, with channels for routing the cables. We join the bones together into a skeleton using rubber band ligaments, and route braided fishing line cables through the channels. We also 3D print a two part mould, and seal it in preparation for casting silicone. To embed the skeleton within the silicone we first cast a layer of silicone into just one half of the mould. We tack the skeleton to this layer using cyanoacrylate, and pour a middle layer of silicone to secure the skeleton in place. We then bolt the second half of the mould on, and pour the remainder of silicone. After curing, we can optionally add small cuts to the robot to refine its shape and stiffness properties. Finally the robot is mounted on a rigid base, and its tendons connected to motors.

This fabrication pipeline is general-purpose and accessible, requiring only a customary FDM printer and off-the-shelf materials. In Section VI we discuss possible extensions of our method, to increase precision and widen the space of fabricable robots to those with complex, nonplanar skeletons.

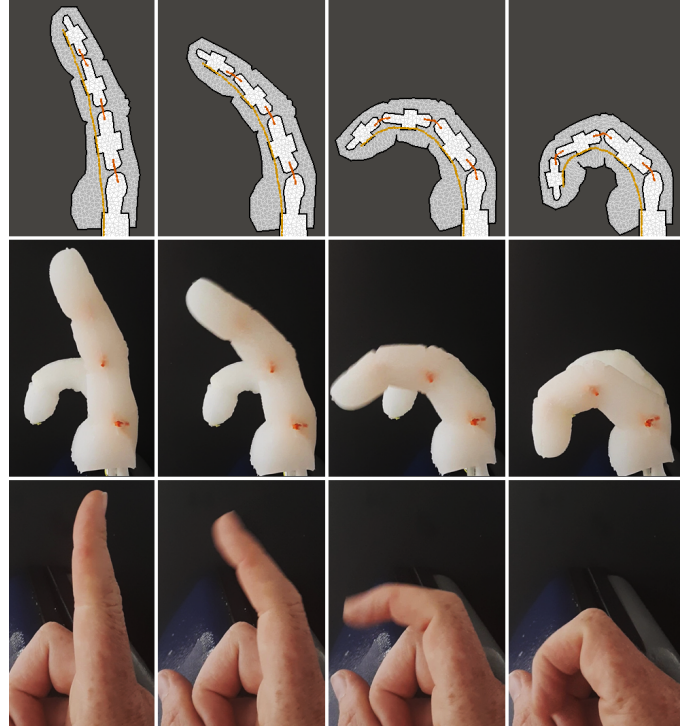


Fig. 4. Single tendon finger bending in simulation (top row) and reality (middle row), along with still images from video of a human finger performing a similar motion (bottom row), demonstrating the capacity for hybrid soft-rigid robots to closely mimic biological systems.

IV. EXPERIMENTS

We perform experiments using real-world hardware to understand the impact of embedded passive skeletal systems (bones and ligaments) on soft robot deformation. In each case we follow the fabrication pipeline described in Section III. Our results demonstrate that skeletons can enhance soft robots’ resistance to external loads and force output. In addition, we set up analogous simulations following the pipeline described in Section II, in order to obtain a qualitative comparison between the behavior of the real-world system and our simulator. We show that these simulations capture the salient features of the robots’ deformed shape—and demonstrate the potential for simulation to inform the design and control of soft robots with internal skeletons—though note that as 2D simulations they do

not provide an absolute prediction of e.g. pushing force for the experiment in Section IV-A.

A. External Load Resistance

To understand how bones and ligaments affect resistance to external loads we bolt the base of a soft EcoFlex finger with bones and ligaments in place and tie a cable through the tip. We pull on the cable with a series of loads, photograph the finger's deformation, and measure the axial displacement of the tip. We repeat this procedure for a finger with bones but no ligaments, and a finger with neither bones nor ligaments. We observe that bones and ligaments significantly increase the finger's ability to resist external loads, and maintain its shape (see Figure 5). Just bones are also effective, though we note that the fingertip displaces further due to the absence of ligaments, and necking is observed in between the bones, particularly the last two. The no bones, no ligament finger deforms easily and smoothly. We confirm our results in simulation (see Figure 6).

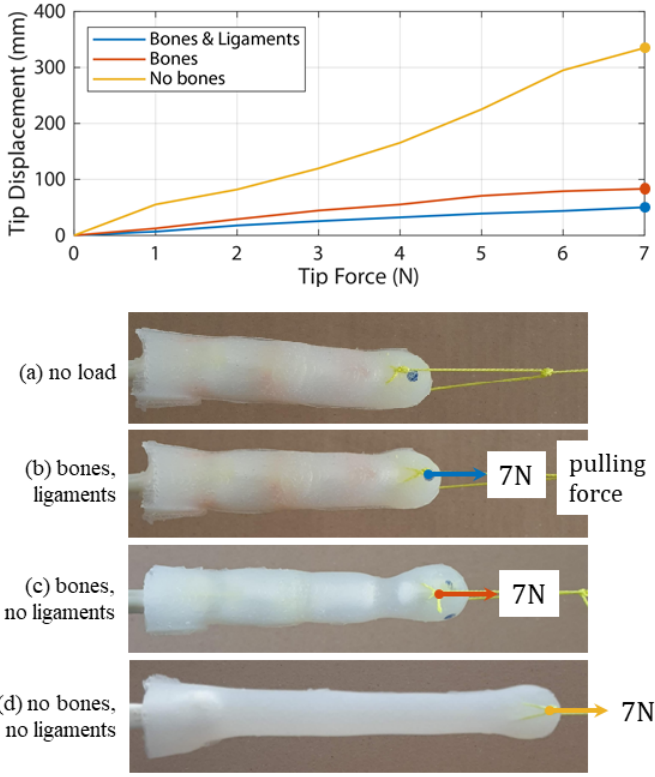


Fig. 5. We show that the addition of internal bones and ligaments can enable soft robots to resist larger external forces. To demonstrate this we bolt the base of a soft finger in place, and secure a cable to its tip. We pull on the cable with increasing force, and plot the resulting tip displacement. We repeat this procedure for three conditions (fingers containing bones and ligaments, bones but no ligaments, neither bones nor ligaments). Snapshots of all three conditions for the same applied tip force are shown in the pictures below, and corresponding dots drawn on the plot.

B. Force Output

To characterize the effect of soft robot skeletal systems on force output, we bolt the base of a soft EcoFlex finger

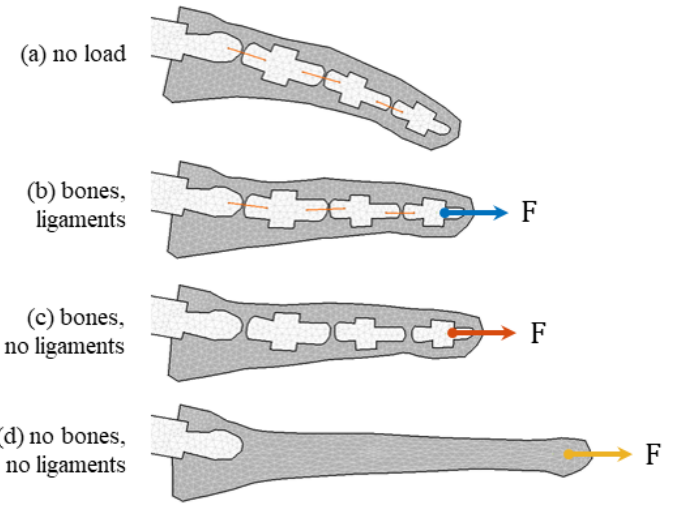


Fig. 6. We evaluate how well our simulation can capture the salient behavior of the pulling experiment. We observe that the bones and ligaments case holds its shape well, the bones and no ligaments case exhibits separation between the final two bones and some necking, and the no bones no ligaments case deforms freely and smoothly, as we observed in reality.

with bones and ligaments into a linear stage. We position a force sensitive resistor (FSR) beneath the finger tip, and drive the finger downwards. We record the pushing force measured by the FSR as the finger is compressed. We also photograph the finger's deformed shape at the maximum recorded compression. We repeat this experiment for a finger with bones but no ligaments, and a finger with neither bones nor ligaments. We observe the addition of bones increases the finger's ability to exert force, and the addition of ligaments increases it still further (see Figure 7).

This is a somewhat surprising result, as this experiment works by applying a compressive load to the finger, which we would not expect to significantly engage the ligaments. Our hypothesized explanation is that the ligaments keep the bones closer together during casting, which leads to a fabricated finger that better resists pushing. We find evidence for this hypothesis using our simulator (see Figure 8).

To simulate the translation of the finger by the test rig, we translate the rest positions of the pin on its topmost nodes. To model the FSR we use the penalty method from [25], where a one-sided quadratic energy is added for each node to resist penetration of the ground. Finally to recover the force exerted on the FSR, we sum the force contribution of this energy over all the nodes, and take the magnitude. Our simulation confirms that bones increase force output, but finds that simply adding ligaments does not increase it further. However if we slightly pretension the added ligaments—as a proxy for the bones being held closer together during fabrication—we find that force output increases, like we observed in the real-world. This highlights the use of simulation as a tool for understanding the real-world behavior of hybrid soft-rigid robots. It also suggests that relatively small variations in fabrication can lead to larger downstream changes in robot behavior, motivating the further development of fabrication pipelines (see Section VI).

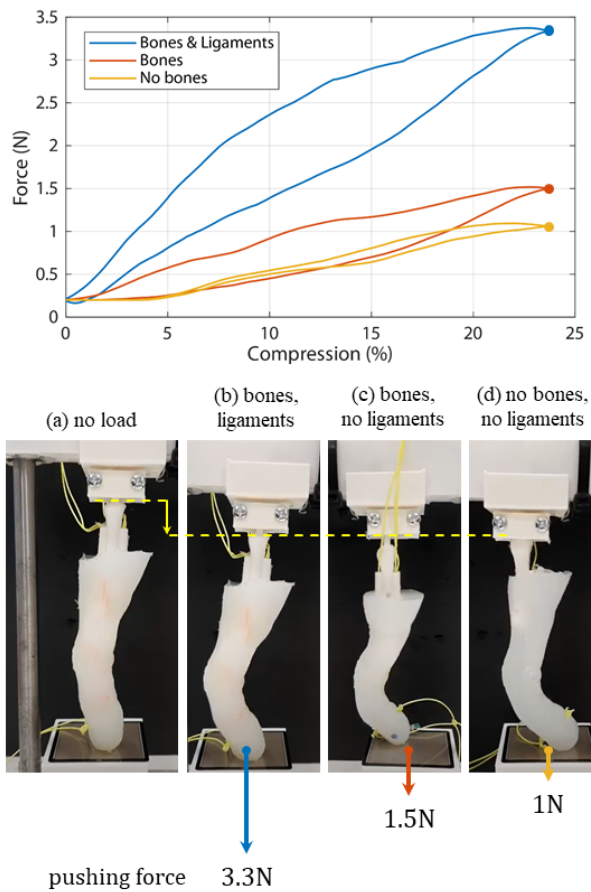


Fig. 7. We show that the addition of bones and ligaments can enable a robot to apply greater force. To demonstrate this we bolt the base of a soft finger into a linear stage, and position a force sensitive resistor (FSR) below it. We drive the finger down (and then back up), and plot the force measured by the FSR. We repeat this procedure for three conditions. Snapshots are shown in the pictures below, with corresponding dots drawn on the plot.

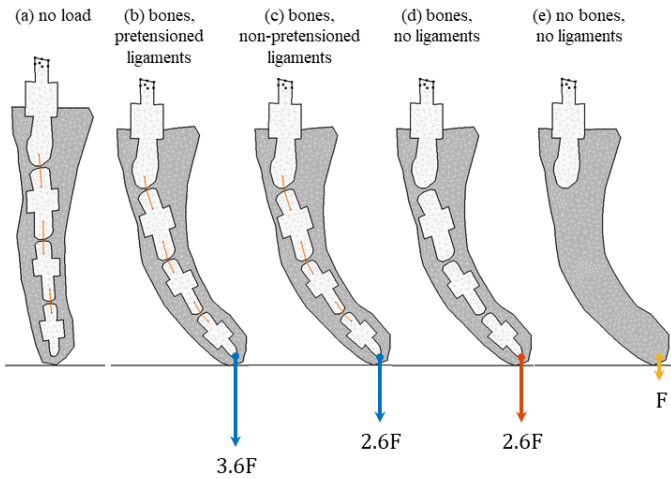


Fig. 8. We evaluate how well our simulation can capture the salient behavior of the pushing experiment. We report net force exerted on the simulated ground (force sensitive resistor) normalized to the no bones, no ligaments case. Our simulation captures the trend that bones increase pushing force, and helps explain why ligaments were observed to increase force output in the real world.

V. APPLICATIONS

We can leverage the strength and predictive power of our fabrication and simulation pipelines to start tackling problems in hybrid soft-rigid manipulation and control.

A. Finger and Hand Prototypes

We fabricate a four-cable hybrid soft-rigid robotic finger, and explore its range of motion in Figure 9. We also build a

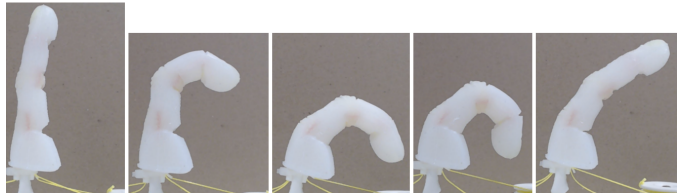


Fig. 9. Poses illustrating the range of motion of a four-cable hybrid soft-rigid robotic finger.

hybrid soft-rigid robotic hand from fingers and a thumb made using our fabrication pipeline. In Figure 10 we show this hand grasping, and performing in-hand manipulation.

B. Soft Finger Trajectory Optimization

Because our simulation method for hybrid soft-rigid robots with internal skeletons is differentiable, we can use it as the inner loop in previously developed methods for Soft IK [27] and trajectory optimization [25]. In Figure 11 we show control sequences found by repeatedly performing Soft IK along a trajectory of targets. Given a target tip position y' , Soft IK finds optimal cable contractions by minimizing the objective $\mathcal{O} = \|y(u) - y'\|^2$. To adapt Soft IK for one of our hybrid soft-rigid fingers, we exclude the ligaments from the optimization, since we cannot control their length. In code this is easily accomplished by setting the corresponding entries of the objective gradient $\frac{\partial \mathcal{O}}{\partial u}$ to zero before performing line search to update the vector of cable contractions u .

VI. DISCUSSION AND FUTURE WORK

A. Fabricating Robots With More Complex Skeletons

As we continue to explore the space of hybrid soft-rigid robots, even more general fabrication pipelines are called for. The examples in this work were all fabricable using our multistep casting process. In the future it would be interesting to extend our fabrication pipeline to produce robots with complex, nonplanar skeletons, like the 3D arm we simulate in Figure 12. Fixturing could be employed to suspend the bones in the mould prior to pouring in silicone or foam. One could leverage techniques from computational design to automatically augment moulds with the geometry required to fixture an input skeleton within them. Another approach would be to leverage 3D printing to produce hybrid soft-rigid robots using a single fabrication process. This could involve multi-material 3D printers [13], [31], [32] or spatially varying lattice geometry [33].



Fig. 10. The full hybrid soft-rigid hand (a) is capable of grasping various objects and performing simple in-hand manipulation tasks. b) shows the range of grasps that can be achieved with c) highlighting some of the in-hand manipulation tasks.

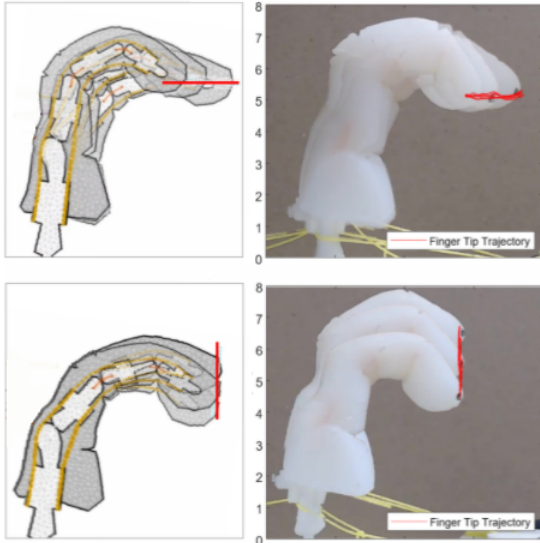


Fig. 11. In simulation (left) we use Soft IK to generate control sequences that trace horizontal (top) and vertical (bottom) target trajectories. On the real four-cable finger (right) we repeat the motion repeated for 5 times. We overlay the resulting tip trajectories on snapshots of the motion.

B. Low-Friction Joint Design

In this work we did not employ explicit joints, instead allowing silicone to infiltrate the space between neighboring bones. However, as we continue to push the limits to which our robots can mimic biology—in terms of both deformation behavior and performance—it would be interesting to develop a more biologically-inspired, low-friction solution to joints. The joints in our body make use of fluid filled sacs called bursae to reduce friction and provide cushioning. It would be exciting to try building and simulating a similar solution.

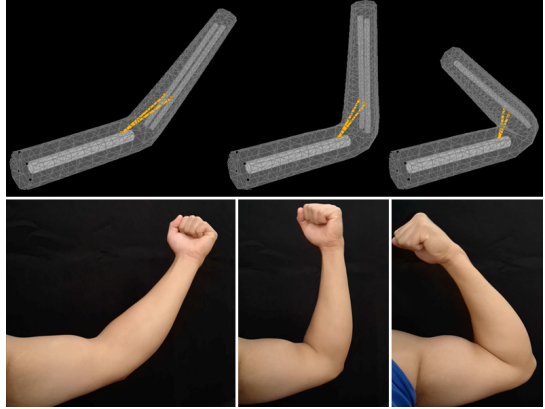


Fig. 12. An exploratory simulation of a 3D bio-inspired hybrid soft-rigid robotic arm with nonplanar skeleton. The top row shows the simulations corresponding to the bottom poses of a human arm.

VII. CONCLUSION

We are at the beginning of an exciting development in the field of soft robotics, with the emerging development of hybrid soft-rigid robots. We presented an investigation into building robots by embedding rigid skeletons inside of soft materials, with foundational, general-purpose pipelines for simulation and fabrication. The addition of bones was shown to increase robot's strength, while supporting the delicacy of movement we see in the natural world. In the future it will be exciting to continue pushing the performance of hybrid robots—increasing strength, and reducing friction—as well as the fidelity with which we can simulate them.

REFERENCES

- [1] M. T. Tolley, R. F. Shepherd, K. C. Galloway, R. J. Wood, and G. M. Whitesides, "A resilient, untethered soft robot," *Soft robotics*, 2014.
- [2] A. Bicchi, G. Tonietti, and E. Piaggio, "Design, realization and control of soft robot arms for intrinsically safe interaction with humans," in *Proc. IARP/RAS Workshop on Technical Challenges for Dependable Robots in Human Environments*, 2002, pp. 79–87.

- [3] M. Raibert, K. Blankespoor, G. Nelson, and R. Playter, "Bigdog, the rough-terrain quadruped robot," *IFAC Proceedings Volumes*, vol. 41, no. 2, pp. 10 822–10 825, 2008.
- [4] C. Freschi, V. Ferrari, F. Melfi, M. Ferrari, F. Mosca, and A. Cuschieri, "Technical review of the da vinci surgical telemomanipulator," *The International Journal of Medical Robotics and Computer Assisted Surgery*, vol. 9, no. 4, pp. 396–406, 2013.
- [5] U. Culha, J. Hughes, A. Rosendo, F. Giardina, and F. Iida, "Design principles for soft-rigid hybrid manipulators," in *Soft robotics: Trends, applications and challenges*. Springer, 2017, pp. 87–94.
- [6] E. Brown, N. Rodenberg, J. Amend, A. Mozeika, E. Steltz, M. R. Zakin, H. Lipson, and H. M. Jaeger, "Universal robotic gripper based on the jamming of granular material," *Proceedings of the National Academy of Sciences*, vol. 107, no. 44, pp. 18 809–18 814, 2010.
- [7] R. Wang, S. Wang, Y. Wang, L. Cheng, and M. Tan, "Development and motion control of biomimetic underwater robots: A survey," *IEEE Transactions on Systems, Man, and Cybernetics: Systems*, 2020.
- [8] B. Xia, J. Fu, H. Zhu, Z. Song, Y. Jiang, and H. Lipson, "A legged soft robot platform for dynamic locomotion," *arXiv preprint arXiv:2011.06749*, 2020.
- [9] M. A. Bell, I. Pestovski, W. Scott, K. Kumar, M. K. Jawed, D. A. Paley, C. Majidi, J. C. Weaver, and R. J. Wood, "Echinoderm-inspired tube feet for robust robot locomotion and adhesion," *IEEE Robotics and Automation Letters*, vol. 3, no. 3, pp. 2222–2228, 2018.
- [10] Y. Tang, Y. Chi, J. Sun, T.-H. Huang, O. H. Maghsoudi, A. Spence, J. Zhao, H. Su, and J. Yin, "Leveraging elastic instabilities for amplified performance: Spine-inspired high-speed and high-force soft robots," *Science advances*, vol. 6, no. 19, p. eaaz6912, 2020.
- [11] J. M. Bern and D. Rus, "Soft ik with stiffness control," in *2021 IEEE 4th International Conference on Soft Robotics (RoboSoft)*. IEEE, 2021, pp. 465–471.
- [12] K. Suzumori, S. Iikura, and H. Tanaka, "Development of flexible microactuator and its applications to robotic mechanisms," in *Proceedings. 1991 IEEE International Conference on Robotics and Automation*. IEEE Computer Society, 1991, pp. 1622–1623.
- [13] Y. Yang, Y. Chen, Y. Li, M. Z. Chen, and Y. Wei, "Bioinspired robotic fingers based on pneumatic actuator and 3d printing of smart material," *Soft robotics*, vol. 4, no. 2, pp. 147–162, 2017.
- [14] M. Jiang, Z. Zhou, and N. Gravish, "Flexoskeleton printing enables versatile fabrication of hybrid soft and rigid robots," *Soft robotics*, vol. 7, no. 6, pp. 770–778, 2020.
- [15] S. Kurumaya, K. Suzumori, H. Nabae, and S. Wakimoto, "Musculoskeletal lower-limb robot driven by multifilament muscles," *Robomech Journal*, vol. 3, no. 1, pp. 1–15, 2016.
- [16] A. A. M. Faudzi, J. Ooga, T. Goto, M. Takeichi, and K. Suzumori, "Index finger of a human-like robotic hand using thin soft muscles," *IEEE Robotics and Automation Letters*, vol. 3, no. 1, pp. 92–99, 2017.
- [17] L. Tian, H. Li, M. F. K. B. A. Halil, N. M. Thalmann, D. Thalmann, and J. Zheng, "Fast 3d modeling of anthropomorphic robotic hands based on a multi-layer deformable design," *arXiv preprint arXiv:2011.03742*, 2020.
- [18] S. Hashemi, D. Bentivegna, and W. Durfee, "Bone-inspired bending soft robot," *Soft Robotics*, 2020.
- [19] O. Goury, B. Carrez, and C. Duriez, "Real-time simulation for control of soft robots with self-collisions using model order reduction for contact forces," *IEEE Robotics and Automation Letters*, vol. 6, no. 2, pp. 3752–3759, 2021.
- [20] J. Hughes, P. Maiolino, and F. Iida, "An anthropomorphic soft skeleton hand exploiting conditional models for piano playing," *Science Robotics*, vol. 3, no. 25, 2018.
- [21] K. Gilday, J. Hughes, and F. Iida, "Wrist-driven passive grasping: interaction-based trajectory adaption with a compliant anthropomorphic hand," *Bioinspiration & Biomimetics*, vol. 16, no. 2, p. 026024, 2021.
- [22] ——, "Jamming joints for stiffness and posture control with an anthropomorphic hand," in *2021 IEEE 4th International Conference on Soft Robotics (RoboSoft)*. IEEE, 2021, pp. 134–140.
- [23] S. Li, J. J. Stampfli, H. J. Xu, E. Malkin, E. V. Diaz, D. Rus, and R. J. Wood, "A vacuum-driven origami ‘magic-ball’ soft gripper," in *2019 International Conference on Robotics and Automation (ICRA)*. IEEE, 2019, pp. 7401–7408.
- [24] S. Li, S. A. Awale, K. E. Bacher, T. J. Buchner, C. Della Santina, R. J. Wood, and D. Rus, "Scaling up soft robotics: A meter-scale, modular, and reconfigurable soft robotic system," *Soft Robotics*, 2021.
- [25] J. M. Bern, P. Banzet, R. Poranne, and S. Coros, "Trajectory optimization for cable-driven soft robot locomotion," in *Robotics: Science and Systems*, vol. 1, no. 3, 2019.
- [26] O. Goury and C. Duriez, "Fast, generic, and reliable control and simulation of soft robots using model order reduction," *IEEE Transactions on Robotics*, vol. 34, no. 6, pp. 1565–1576, 2018.
- [27] J. M. Bern, G. Kumagai, and S. Coros, "Fabrication, modeling, and control of plush robots," in *2017 IEEE/RSJ International Conference on Intelligent Robots and Systems (IROS)*. IEEE, 2017, pp. 3739–3746.
- [28] J. R. Shewchuk, "Triangle: Engineering a 2d quality mesh generator and delaunay triangulator," in *Workshop on Applied Computational Geometry*. Springer, 1996, pp. 203–222.
- [29] H. Si, "Tetgen, a delaunay-based quality tetrahedral mesh generator," *ACM Transactions on Mathematical Software (TOMS)*, vol. 41, no. 2, pp. 1–36, 2015.
- [30] M. Li, Z. Ferguson, T. Schneider, T. Langlois, D. Zorin, D. Panozzo, C. Jiang, and D. M. Kaufman, "Incremental potential contact: Intersection-and inversion-free, large-deformation dynamics," *ACM transactions on graphics*, 2020.
- [31] L.-K. Ma, Y. Zhang, Y. Liu, K. Zhou, and X. Tong, "Computational design and fabrication of soft pneumatic objects with desired deformations," *ACM Transactions on Graphics (TOG)*, vol. 36, no. 6, pp. 1–12, 2017.
- [32] M. Skouras, B. Thomaszewski, S. Coros, B. Bickel, and M. Gross, "Computational design of actuated deformable characters," *ACM Transactions on Graphics (TOG)*, vol. 32, no. 4, pp. 1–10, 2013.
- [33] J. Panetta, Q. Zhou, L. Malomo, N. Pietroni, P. Cignoni, and D. Zorin, "Elastic textures for additive fabrication," *ACM Transactions on Graphics (TOG)*, vol. 34, no. 4, pp. 1–12, 2015.